DE GRUYTER OPEN

Journal of MECHANICAL ENGINEERING – Strojnícky časopis,
VOL 67 (2017), NO 2, 37 - 50

STU SjF

ULTRASONIC DEFECT DETECTION OF STRUCTURAL PLATES USING QUASI-RAYLEIGH WAVES

HLAVATÝ Michal[1], STAREK Ladislav[1], MUSIL Miloš[1], HUČKO Branislav[1]

[1]*Slovak University of Technology in Bratislava, Faculty of Mechanical Engineering, Institute of Applied Mechanics and Mechatronics, Nám. slobody 17, 812 31 Bratislava, Slovakia, email: milos.musil@stuba.sk*

Abstract: This article discusses the application of so-called ultrasonic quasi-Rayleigh waves to detect surface defects of mechanical constructions, namely plate structures. The application of quasi-Rayleigh waves allows the extension of the scope of detection using conventional ultrasonic methods that are based on bulk waves. This extension means larger distances as well as higher sensitivity of the detection of surface defects such as fatigue or corrosion cracks. An advantage of this method is the transfer of wave energy from one side of a plate to another, which helps to overcome one-sided obstacles (such as cross-pieces, reinforcement elements). The article describes characteristic properties of quasi-Rayleigh waves that are important for the proper (in terms of frequency in particular) design of the excitation of waves towards the structure. FEM simulation results then provide information regarding the sensitivity of the wave response to the presence and sizes of surface defects (perpendicular slots) in an isotropic material with the properties of steel. The theoretical knowledge is set against experimental measurements obtained with the use of a steel plate with cross-pieces welded to it.

KEYWORDS: ultrasonic, quasi-Rayleigh waves, dispersion curves, finite element method, angle beam wedges, steel plate

1 Introduction

Ultrasonic methods used to detect defects of mechanical constructions have been widely used and proven for several decades. They are used in the detection of faults in critical structural points, e.g. welds or rails. The assessment of presence of a certain defect is based on the measurement of response to the excitation of longitudinal and traverse (shear) bulk waves. The main drawback of those methods is a relatively high rate of attenuation with distance and interaction with surface elements, which cause the reflection of waves and thus make the assessment of wave response more complicated. This is why their use is limited to the examination of local, relatively small structural parts.

Recently, one area of focus for development has been the use of guided waves that are able to propagate over longer distances with relative low wave energy losses. Central to the research is the capability of such waves to respond to the occurrence of a particular fault and then transmit the indication to a wave sensing point. The main impediment in the development and application of those methods is the fact that guided waves are able to exist only in materials with certain cross-sectional shapes (beams, panels, bars). One type of guided waves is quasi-Rayleigh waves as a group of Rayleigh-Lamb waves. Quasi-Rayleigh waves are able to propagate in flat structural members (Fig.1), whether straight or rounded.

Plate elements have many uses in practice, including aircraft structures, pressure vessels, load-carrying members, etc. Quasi-Rayleigh waves lend themselves to the detection of surface defects in such parts, even over extended distances. Their great benefit is the ability of guided wave energy transmission between the sides of a plate with which it is possible to overcome unilateral structural obstacles.

DOI: 10.1515/scjme-2017-0016, Print ISSN 0039-2472, On-line ISSN 2450-5471 ©2017 SjF STU Bratislava

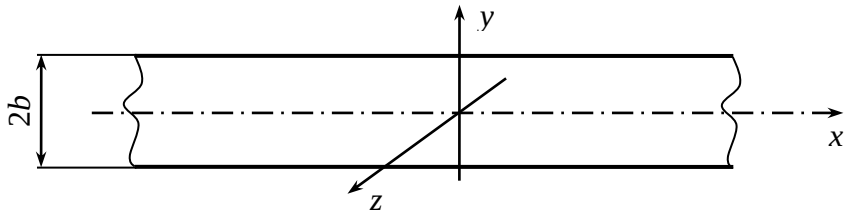

Fig. 1 Infinite plate model

2 Theoretical description of quasi-Rayleigh waves

Quasi-Rayleigh wave is the name given to a sum of the fundamental symmetric (S_0) and anti-symmetric (A_0) mode of Rayleigh-Lamb waves for a certain value of the frequency-thickness product (f *2b) of a plate. These are the values at which the wavenumber curves of the symmetric and anti-symmetric modes are markedly converged (Fig.2). Then, the sum of the two modes is very similar to a Rayleigh wave propagating in an infinite half-space (Fig.3).

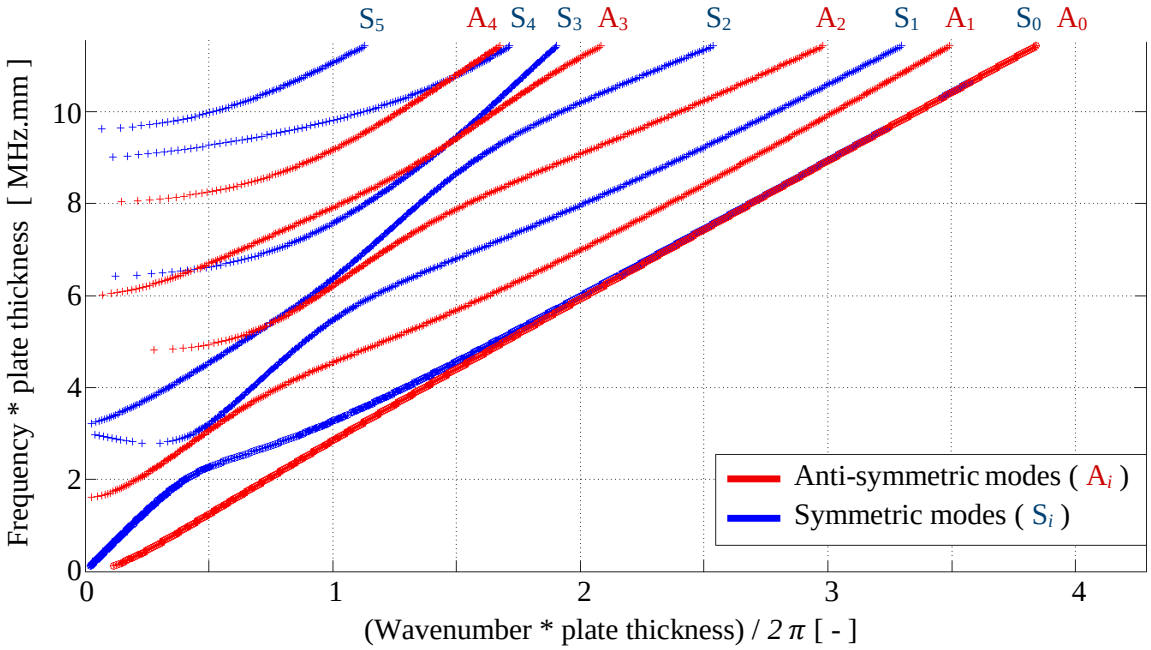

Fig. 2 Dispersion curves of real wavenumbers for steel properties

The infinite-half space (infinite thickness plate) condition is not realistic. When the material is excited (e.g. by means of an end wedge), the Rayleigh waves immediately start to decompose into separate S_0 and A_0 modes. The rate of this decomposition depends on the frequency-

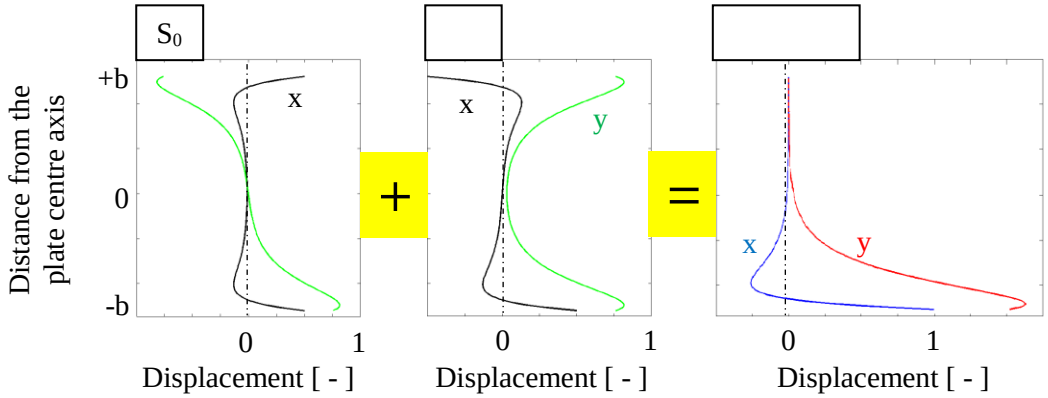

Fig. 3 Summation of the amplitudes of fundamental A_0 and S_0 mode displacements (*x* and *y* coordinates as per Fig.1)

thickness product, f_0*2*b*. When this value is sufficiently high or the propagation distance small, the decomposition is practically negligible. In such case, the waves can directly be considered as Rayleigh waves with properties similar to those occurring in an infinite half-space. Where the decomposition of waves cannot be disregarded, the waves are referred to as quasi-Rayleigh waves. This means that the superposition of the S_0 and A_0 waves is very similar to Rayleigh waves, while they have different propagation properties.

The propagation of quasi-Rayleigh waves is affected by dispersion, i.e. the function between phase / group velocity and wave frequency. The S_0 wave always has a phase velocity that is higher than that of the A_0 wave, and the S_0 wave thus propagates a phase ahead of the A_0 wave. This is accompanied by a change of the final sum of the S_0 and A_0 modes (Fig.4). The change is periodical and is characterised by the transmission of the main wave energy between the upper and lower sides of the plate. The distance over which the phase shift value reaches 2π is called 'beat-length' and it is calculated as follows [12]:

$$L_b = \frac{2\pi}{\xi_{A_0} - \xi_{S_0}} \tag{1}$$

where ξ_{So} is the wavenumber of the symmetric mode (S_0)

ξ_{Ao} is the wavenumber of the anti-symmetric mode (A_0)

(common frequency for ξ_{So} and ξ_{Ao})

The wave energy maxima on the lower side of the plate are located at the distance L_b from the point of excitation and at its multiples (Fig. 4). On the contrary, wave energy maxima on the other, upper side of the plate are located at half distances of the multiples of L_b. Energy

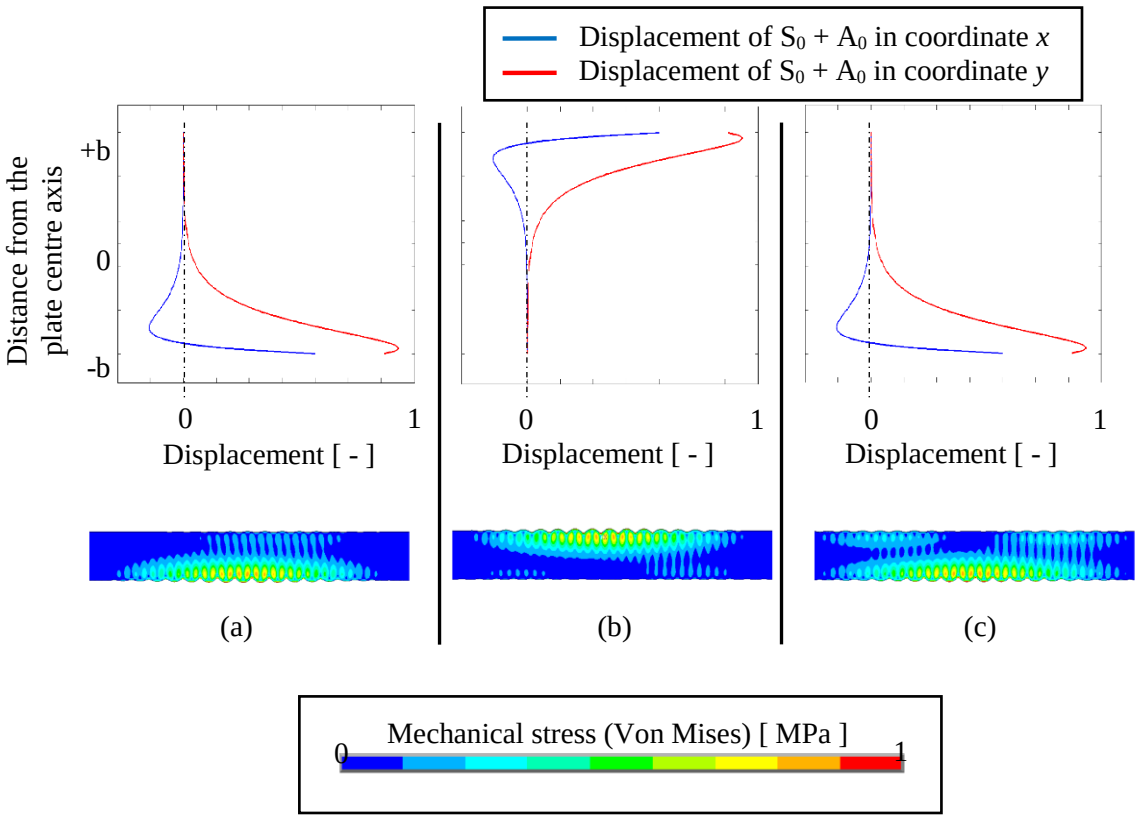

Fig. 4: Representation of the resulting $S_0 + A_0$ modes and of (von Misses) stresses at FEM model (simulation of quasi-Rayleigh wave propagation) at distance x from the starting point of propagation: (a) $x = 0$ m; (b) $x = L_b/2$; (c) $x = L_b$

exchange between the two sides of the plate is fluent, since phase velocities remain the same. The upsetting of the resulting amplitudes is a useful property that allows the overcoming of one-side obstacles and the two-side observation of surface damage in a plate structural element.

The character of the wave energy transmission in real samples is indicated by the peak-to-peak signal amplitude along two plates of the same thickness, one even plate and one plate with cross-pieces (Fig.5). Waves produce a 20-cycle impulse with the fundamental frequency of 1.55 MHz, modulated by the Hann window. The excitation is provided and sensed by a pair of angle beam wedge transducers using the pitch–catch technique for measurement. The peak-to-peak amplitude of the signal in the central portion of the impulse is captured at given distances from the excitement point.

With regard to theoretical assumptions, the amplitude maxima at the upper side of the plate are located at distances $l \approx L_b$, $2L_b$ (the wave excitation occurs on the upper side). The situation on the lower side is just the opposite. The actual value of L_b agrees well with the theoretical value. The proposal of suitable excitement frequency confirms the similarity of peak-to-peak amplitudes of the even plate and the cross-piece plate. This means that there is small attenuation in the cross-piece area.

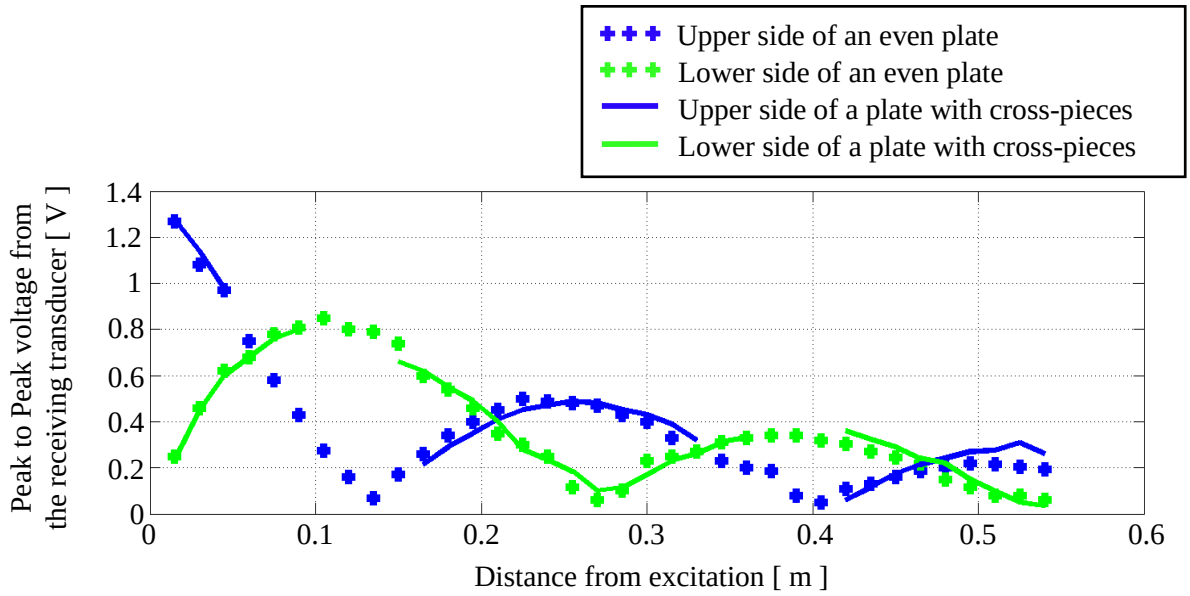

Fig. 5: Comparison of the peak-to-peak amplitudes of waves for an even plate and a cross-piece plate of the same thickness (f = 1.55 MHz; 20-cycle Hann modulation; $L_b \approx 0.2774$ m); the thickness of cross-pieces is the same as the plate thickness and the distances of the cross-pieces from the transducer are 0.135 m and 0.405 m.

3 Finite element analysis

3.1 Finite element model

FEM (Ansys) simulations are performed to determine the theoretical interaction of quasi-Rayleigh waves with an existing defect. A physical 2D model of the plate (with properties of steel; Tab.1) has been made for that purpose. The modelling principles differ from those used in structural analysis modelling. In order to ensure a sufficiently precise calculation of wave propagation, an 8-node plane element (PLANE 183, plane strain problem) was used having the max. size of a side as follows [4]:

$$\Delta l = \frac{\lambda_{min}}{20} \tag{2}$$

where λ_{min} is the lowest considered wavelength of the wave.

Tab.1: Considered material properties of steel

Density	ρ = 7850 kg.m^{-3}
Young´s modulus	E = 2.1x10^{11} MPa
Poisson´s ratio	ν = 0.3

The time step is as follows:

$$\Delta t \leqq \frac{1}{20\, f_{max}} \tag{3}$$

where f_{max} is the highest considered wave frequency.

Moreover, the time step must be designed so that the calculation generates an acceptable period error due to numerical dispersion. For the Newmark algorithm or, more accurately, the average acceleration method, the period errors will be calculated as shown below [5]:

$$\frac{T_{MKP} - T}{T} = \frac{(2\pi f_{max})^2 \, \Delta t^2}{12} \tag{4}$$

where T_{FEM} is the wave period calculated using FEM

T is a theoretical wave period value

The following parameters have been derived from the previous functions and applied to the given wave impulse frequency range (f = 1.315 MHz, 5-cycle Hann modulation):

- Δl = 8.38 x 10^{-5} m (finite element size)
- Δt = 7.016 x 10^{-9} s (time step)

The dimensions of the physical FEM model are represented in Fig.6. The model size on the left-hand side is reduced for optimisation reasons (to fasten the simulation calculation). Also, the position of the kinematic excitation (5-cycle harmonic impulse in a Hann window) which produces the desired wave is shifted. The wave within the plate is designed with regard to the phase shift between the S_0 and A_0 modes. The wave energy maximum of quasi-Rayleigh waves thus falls to the location of the slot (in distance L_b). Then, there is maximum probability for detection of slot present (type of surface defect).

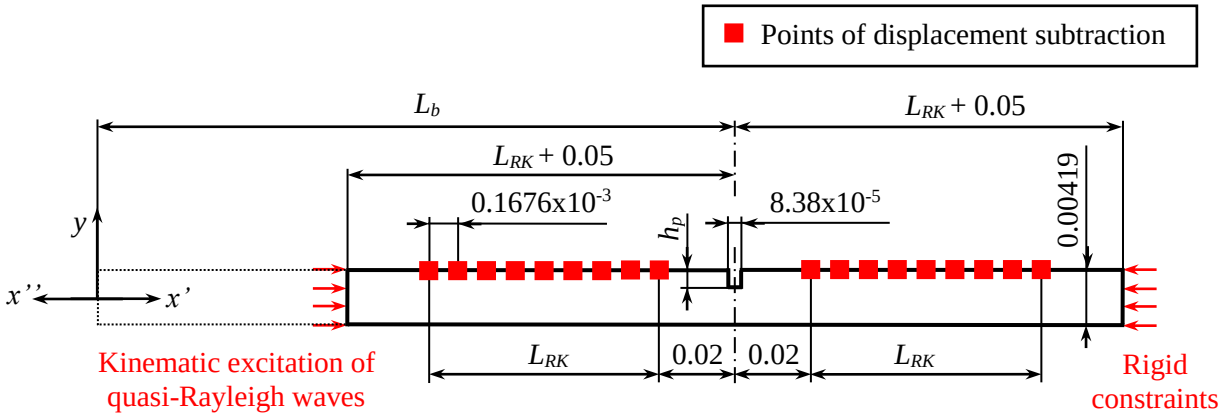

Fig.6 FEM simulation model diagram (the *x'* axis reflects the subtraction of incident waves and transmitted waves; the *x''* axis reflects the subtraction of reflected waves); dimensions are expressed in metres.

The red points on the upper side of the plate (Fig.6) represent the points of subtraction of *y* displacements for the calculation of dispersion coefficients. The dispersion coefficient expresses the ratio of wave component amplitudes after and before the incidence. S_0 (A_0) wave reflection coefficient [4]:

$$R_{f_0}^{S_0\,(A_0)} = \frac{\sum_{j=0}^{O-1}\sum_{k=0}^{P-1} u_{(j,k)}^{R}\, exp\left(-i2\pi\left(\frac{l_{S_0(A_0)}\, j}{O} + \frac{m_{f_0}\, k}{P}\right)\right)}{\sum_{j=0}^{O-1}\sum_{k=0}^{P-1} u_{(j,k)}^{I}\, exp\left(-i2\pi\left(\frac{l_{S_0(A_0)}\, j}{O} + \frac{m_{f_0}\, k}{P}\right)\right)} \tag{5}$$

S_0 (A_0) wave transmission coefficient:

$$T_{f_0}^{S_0\,(A_0)} = \frac{\sum_{j=0}^{O-1}\sum_{k=0}^{P-1} u_{(j,k)}^{T}\, exp\left(-i2\pi\left(\frac{l_{S_0(A_0)}\, j}{O} + \frac{m_{f_0}\, k}{P}\right)\right)}{\sum_{j=0}^{O-1}\sum_{k=0}^{P-1} u_{(j,k)}^{I}\, exp\left(-i2\pi\left(\frac{l_{S_0(A_0)}\, j}{O} + \frac{m_{f_0}\, k}{P}\right)\right)} \tag{6}$$

where $u^R_{(j,k)}$ is the time-distance matrix of displacements of the reflected wave [-]
$u^T_{(j,k)}$ is the time-distance matrix of displacements of the transmitted wave [-]
$u^I_{(j,k)}$ is the time-distance matrix of displacements of the incident wave [-]

O is the number of subtraction points
P is the number of time samples of the signal
$l_{So(Ao)}$ is the integer value of order of the spectral component for ξ_{So} / ξ_{Ao}:

$$l_{S_0(A_0)} = \frac{\xi_{S_0(A_0)}\, L_X}{2\pi}\, O \tag{7}$$

m_{f0} is the integer value of order of the spectral component for f_0:

$$m_{f_0} = f_0\, T_{RK} \tag{8}$$

f_0 is the fundamental wave frequency [Hz]
T_{RK} is the duration of the wave from the point of subtraction [s]

The purpose of calculation of dispersion coefficients is to quantify the reflected and transmitted components of a quasi-Rayleigh wave as a function of the depth of the slot. Hence it expresses the sensitivity of the wave response to the occurrence and size of the given mechanical damage in the model.

3.2 Results of finite elements analysis

Simulations were made for six depths of the mechanical damage (a perpendicular slot) within the range of 4% to 28 % of the plate thickness. The values were then applied to calculate the dispersion coefficients for the length $L_{RK} \approx 0.0114$ m ($L_X = 0.1676\text{x}10^{-3}$ m) and duration $T_{RK} \approx 17.47$ μs. The coefficient values were calculated for each slot depth, as shown in Fig.7 (the wave frequency is f_0 = 1.315 MHz). The graphs indicate changes in the coefficient from the smallest slot depth, i.e. $h_p\,/2b$ = 0.04 (4% of the plate thickness). This confirms the possibility of early detection of the type of fault concerned in the point at the length L_b from the excitement. The coefficients calculated for S_0 and A_0 are nearly identical, which is because of the nearly identical waveforms of the S_0 and A_0 modes as they produce practically the same interaction with the fault. The sum of squared dispersion coefficients expresses the summary energy of the reflected Rayleigh wave and the transmitted Rayleigh wave signals. As follows from Fig.7, at $h_p\,/2b$ = 0.2, nearly a half of incident energy is transformed into kinds of energy other than quasi-Rayleigh wave.

In the other frequency case, at f_0 = 1.531 MHz, the coefficient trend is as shown in Fig.8. The values are very similar to those of the previous case up to the depth $h_p\,/2b$ = 0.1. As the slot depth increases, the dispersion coefficient trend changes. This means that the amount of reflected wave energy is lower, while the amount of transmitted wave energy has temporarily increased. The difference in the dispersion coefficient trend is caused by the proximity of the frequency (f_0) of 1.531 MHz to the so-called cut-off frequency at which quasi-Rayleigh waves are transformed into standing horizontal shear waves (Fig.9). Cut-off frequencies are the points in the dispersion curves (Fig.10) where the group velocity of Rayleigh-Lamb wave modes is zero. These modes form exclusively longitudinal or shear horizontal (SH) standing waves that are irrelevant to the detection. Their exact values can be determined, for example, using the expressions in [11].

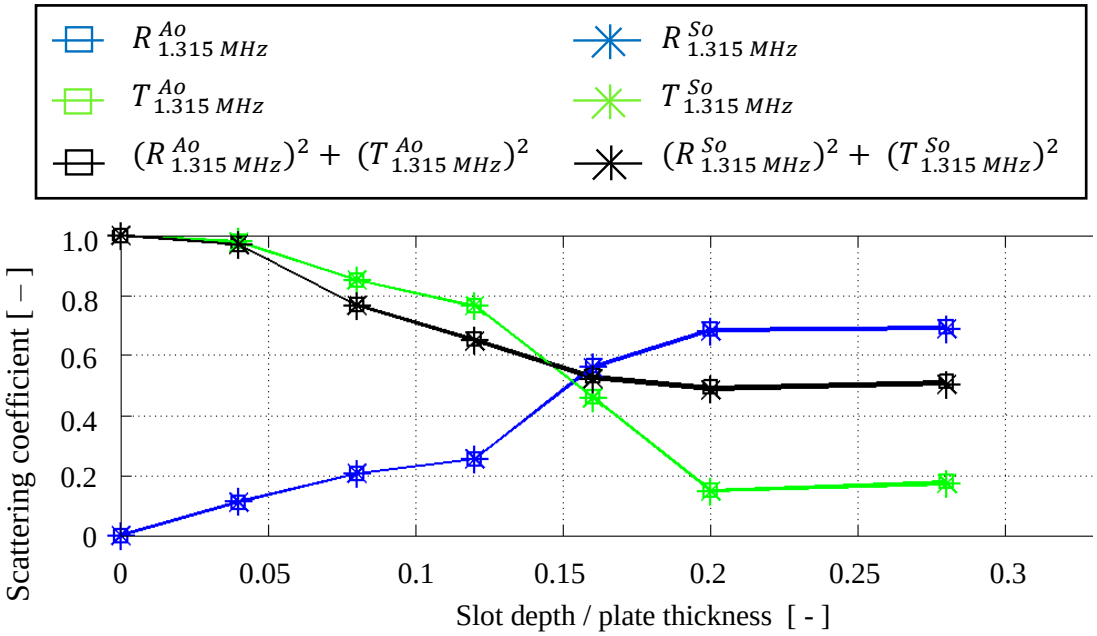

Fig.7 Dispersion coefficient trend for the wave frequency (f_0) of 1.315 MHz, 5-cycle Hann modulation

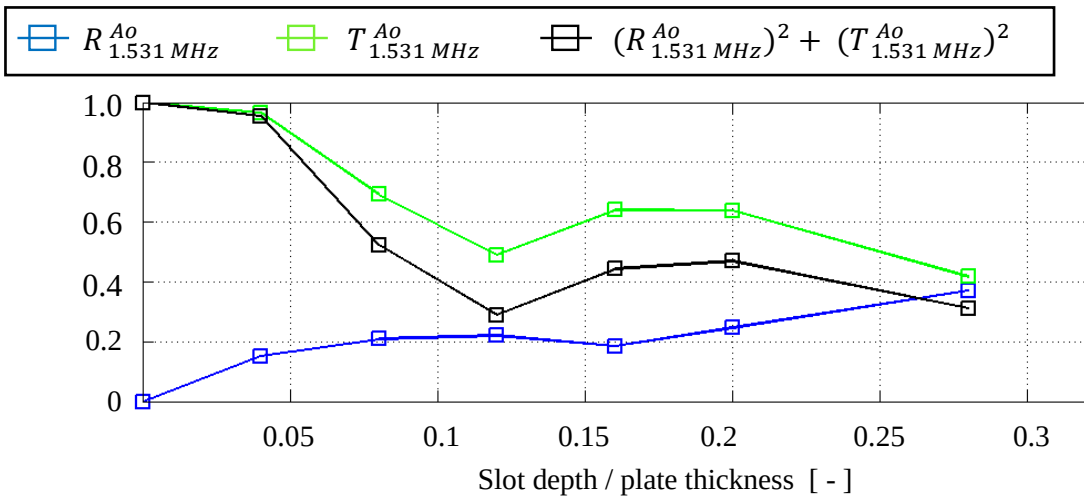

Fig.8 Dispersion coefficient trend for f_0 = 1.531 MHz, 20-cycle Hann modulation

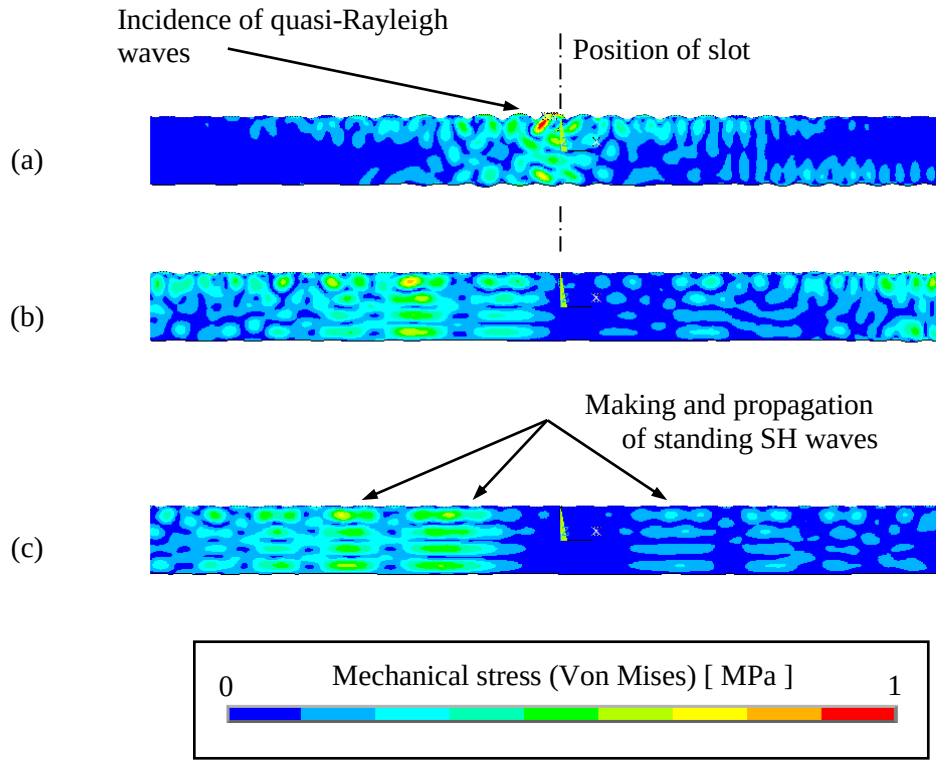

Fig.9 Interaction of a quasi-Rayleigh wave (f_0 = 1.531 MHz, 20 cycles) and a perpendicular slot (h_p = 0.838 mm): (a) time: 45 μs; (b) time: 55 μs; (c) time: 60 μs

The presence of cut-off frequencies and the formation of further symmetric and anti-symmetric modes make the interaction of waves with a defect mode complex. The dispersion coefficient trends become dependent on the wave frequency, which complicates the quantification of the slot depth. When impulse excitation is used, the number of its cycles should ensure that the frequency width covers a sufficient band on the vertical axis, e.g. at least 1 MHz.mm (for the two previous simulation cases). This will ensure the reflection of

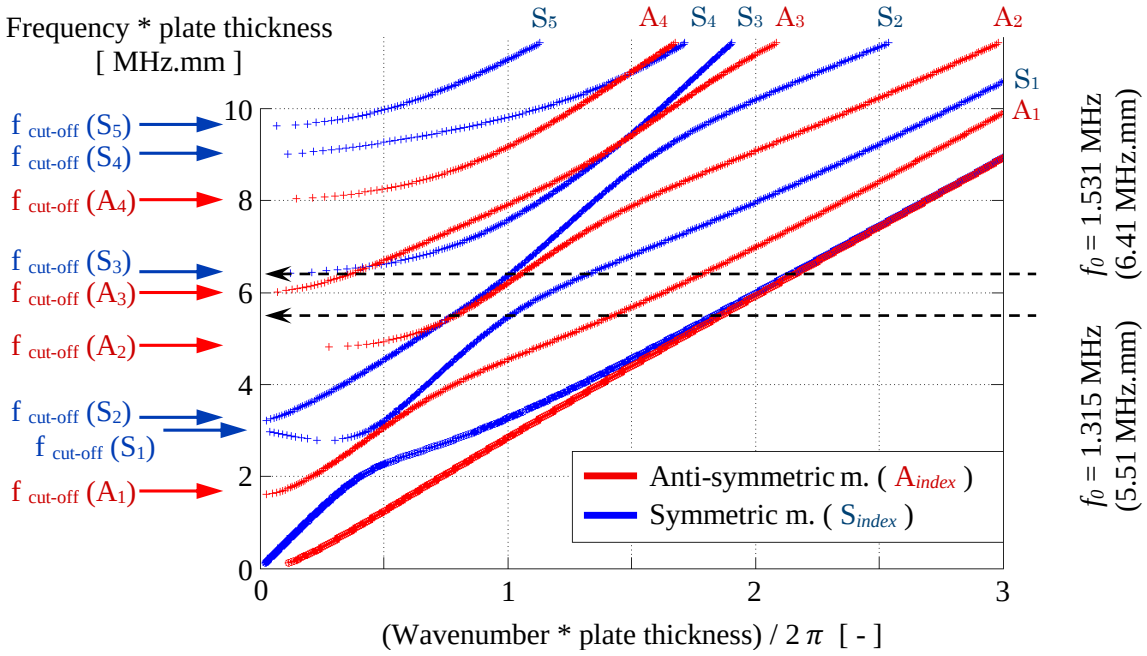

Fig.10 Cut-off frequency values and simulation values marked in the dispersion curve

a sufficiently high relative energy of quasi-Rayleigh waves from the defect to avoid nearly exclusive transformation to other kinds of energy within the cut-off frequency. This will allow the detection of the defect as such, though the approximate quantification of the size (depth) of the slot will be possible only for h_p /2b < 0.1 when the dispersion coefficient trend is independent of frequency. In this case, the notable generation of shear waves and longitudinal waves seen in Fig. 9 [11] does not yet occur.

4 Experimental results

The experimental detection of a perpendicular slot was performed with two steel plates with cross-pieces welded on them (which were measured separately by means of the reflection (pulse-echo) – transmission (pitch-catch) method). The weld penetration depth does not exceed a half of the plate thickness, so the opposite side is even. The generation and measurement of ultrasonic quasi-Rayleigh waves are made by means of angle beam wedge transducers (Fig.11). In both samples the plate thickness is approximately twice the wavelength of quasi-Rayleigh waves.

Fig. 11 Model position of transducers on the sample
for the transmission measurement method

For comparison: The experimental detection is made with two impulse durations (20-cycle and 5-cycle Hann modulation). In the reflection method exercise, the sample plate thickness is 5.2 mm and the fundamental impulse frequency is f_0 = 1.17 MHz (L_b ≈ 0.27 m). The mechanical damage is produced by cutting the plate and measurements are made for slot depths ranging from 0.15 mm to 2.55 mm (h_p /2b = 0.029 to 0.49). The damage is located behind a cross-piece (Fig.12), at a distance of approx. 0.27 m from the transducer. Fig. 13 shows the amplitudes of filtered signals. A rise in the amplitudes of reflected quasi-Rayleigh waves is observed in the case of the smallest slot depth. For both cycle numbers the frequency width of the main lobe is higher than 1 MHz.mm, which ensures sufficient generation

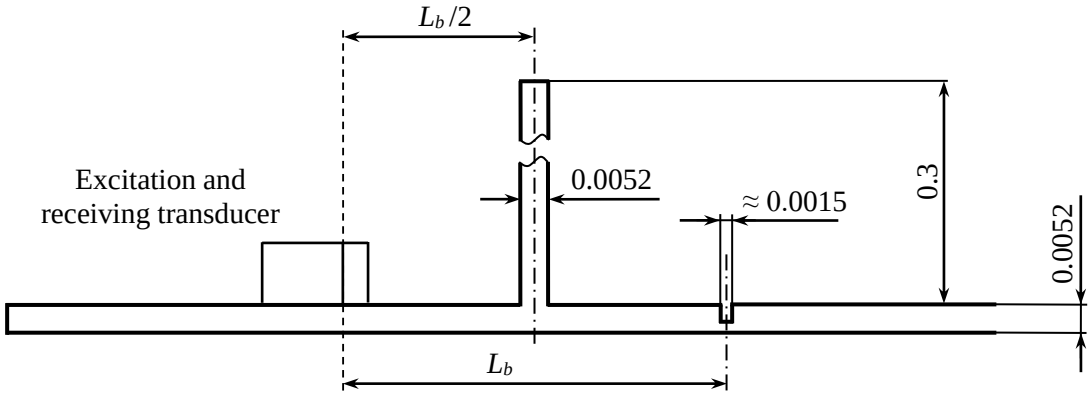

Fig.12 Diagram of sample dimensions and transducer location for the reflection method

of quasi-Rayleigh waves above the noise level of 5 mV. The peak-to-peak amplitude of the incident wave is approx. 430 mV. A moderate decrease in peak-to-peak amplitude values is observable in the area where $h_p/2b = 0.15$, which is similar to the simulation results in Fig.8. This interim decrease is due to the presence of cut-off frequencies, $f_{cut\text{-}off}\ (A_3)$ and $f_{cut\text{-}off}\ (S_3)$ with the values of 1.15 MHz and 1.23 MHz, respectively. Their effect (making of standing longitudinal and shear waves) is, however, insignificant for depths up to $h_p/2b = 0.1$ (Fig.13), which is also mentioned in [11]. This does not restrain the early detection of a cut. An analysis of the incidence time of reflected waves confirmed the position of the slot at a distance of approx. 0.27 m (Fig.14).

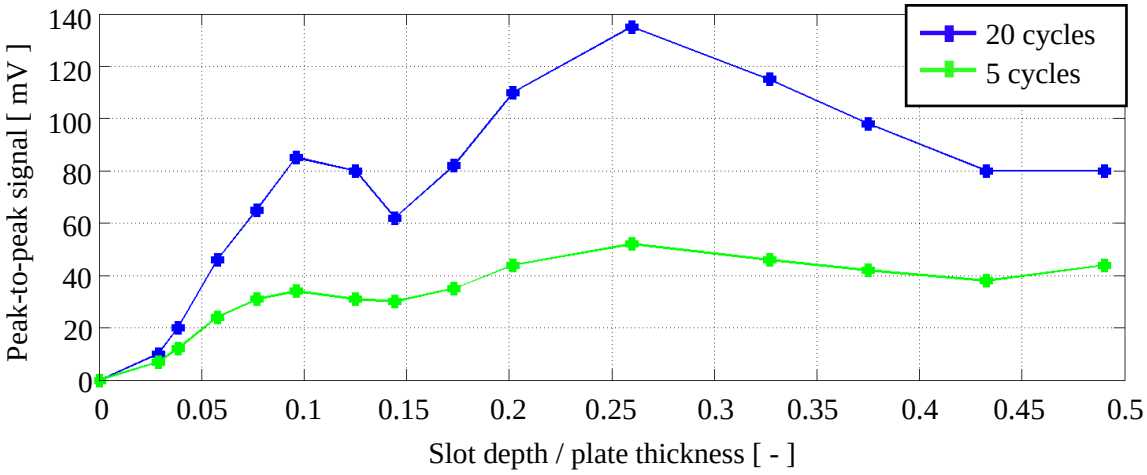

Fig.13 Reflection method: peak-to-peak amplitudes as a function of slot depth / plate thickness ratio for a 20-cycle impulse and a 5-cycle impulse

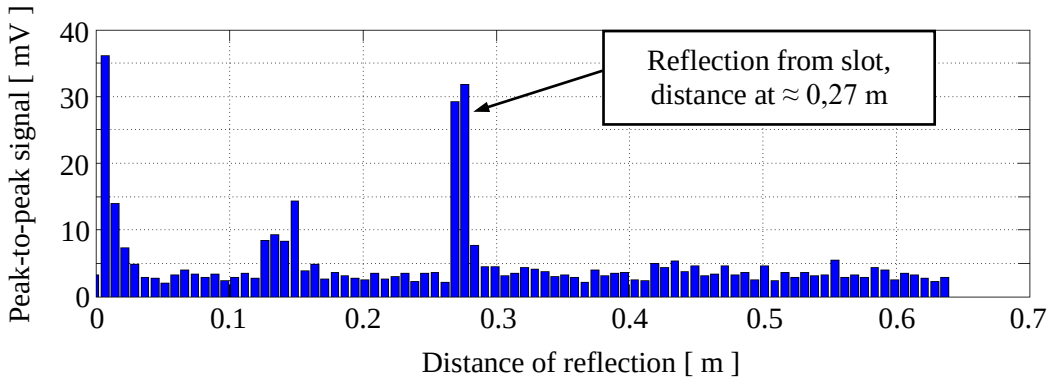

Fig.14 Peak-to-peak amplitudes as a function of the propagation distance of waves (5-cycle impulse)

The transition measurement method was applied to another test sample, i.e. a welded plate of 4.19 mm in thickness, as shown in the scheme in Fig.15. The fundamental frequency of excited waves is $f_0 = 1.55$ MHz. The beat length value predetermined by this plate thickness-frequency configuration is approx. 0.27 m, which is similar to the reflection method (the verification measurement results are shown in Fig.5).

The depth of the perpendicular slot is within the range from 0.15 to 2.3 mm ($h_p/2b = 0.036$ to 0.55). The trend of the measured signal peak-to-peak amplitudes as a function of slot depth is represented in Fig.16. For both numbers of cycles, the slot of peak-to-peak amplitude decrease remains approximately the same until $h_p/2b = 0.07$. From that point, this parameter

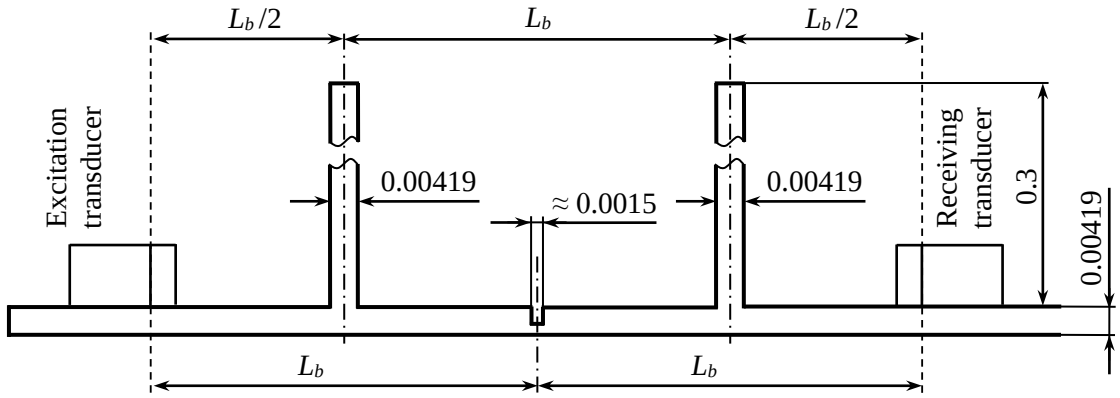

Fig.15 Diagram of sample sizes and transducer locations for the transmission method

starts to decrease markedly to reach a steady value (< 50 mV). For the 20-cycle impulse, a temporary moderate increase in the peak-to-peak amplitude is observed in the area where $h_p/2b$ = 0.2 (due to the influence of cut-off frequencies, similar to Fig.8).

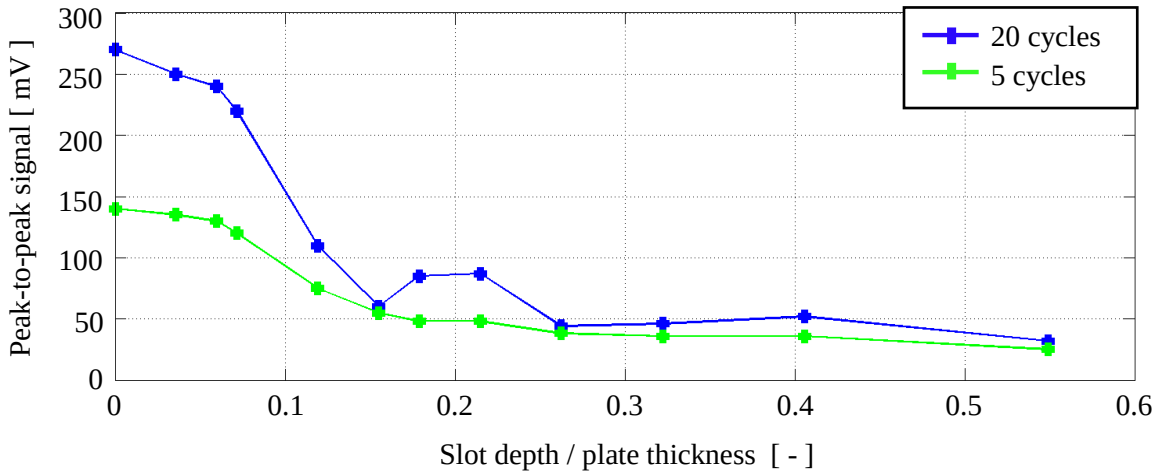

Fig.16 Transmission method: peak-to-peak amplitudes as a function of $h_p/2b$, for a 20-cycle impulse and a 5-cycle impulse

The obvious peak-to-peak amplitude decrease from the lowest slot depth case confirms the theoretical assumptions regarding significant sensitivity of transmitted Rayleigh waves to the presence of a perpendicular slot. The observation of the peak-to-peak amplitude of transmitted waves offers an identical surface damage detection capacity as the reflection method. The effects of cut-off frequencies impeding or preventing the estimation of the defect depth are also present.

5 CONCLUSIONS

The outcomes of the analysis and comparison of theoretical simulations and experimental measurements confirm the high sensitivity of response of quasi-Rayleigh waves to the presence of a surface defect. In both cases, for simulations and measurements, there is similarity of the scattering coefficients trends. 'Defect' in this case refers to discontinuity in the even surface of a plate with a step interface (corrosion or fatigue cracks or other failure). The suitability of quasi-Rayleigh waves for the detection of surface defects follows from the concentration of the main wave energy close to plate surface. Experimental measurements have proven the capacity to detect a defect for slot depth to plate thickness ratios below 5%.

This sensitivity has been proven for both the reflection and transmission methods of measurement. As a condition for this detection capacity, the defect must be present within the area where the maximum wave energy is reached, i.e. the area with the highest sum of the S_0 and A_0 mode amplitudes with a phase shift of $n*\pi$ (where n = 1,2, ...) – Fig.4.

The mechanism of interaction of quasi-Rayleigh waves with an existing defect is not independent of frequency. This means that the peak-to-peak amplitudes of reflected and transmitted waves as functions of defect depth (Fig.13, Fig.16) will slightly vary with different wave frequencies. The reason is the complexity of incident wave dispersion, meaning that further Rayleigh-Lamb wave modes are formed and cut-off frequencies are involved. With this, it is very difficult to quantify the size of a defect by means of the current peak-to-peak amplitude value.

REFERENCES

[1] L. Écsi, P. Élesztős, R. Jančo. On the stress solution of hypoelastic material based models using objective stress rates, *APLIMAT 2016 - 15th Conference on Applied Mathematics 2016, Proceedings, Bratislava, 2 - 4 February* **2016**, 280 - 297, ISBN 978-802274531-4.

[2] K. Frydrýšek, R. Jančo. Simple planar truss (linear, nonlinear and stochastic approach), *Journal of Mechanical Engineering - Strojnícky časopis* **2016** (66), No. 2, 5 - 12, DOI: 10.1515/scjme-2016-0013.

[3] K. F. Graff. Wave motion in elastic solids, Oxford university press, London, **1975**, ISBN-13: 978-0486667454.

[4] F. Moser, L. J. Jacobs, J. Qu. Application of finite element methods to study transient wave propagation in elastic wave guides, Progress in Quantitative Non-destructive Evaluation, Vol l7, Plenum Press, New York, **1998**, ISBN 978-1-4615-5339-7.

[5] M. Géradin, D. Rixen. Mechanical Vibrations: Theory and Application to Structural Dynamics (second edition), John Wiley & Sons, **1997**, ISBN 13: 9780471975465.

[6] M. Castaings, E. Le Clezio, B. Hosten. Modal decomposition method for modelling the interaction of Lamb waves with cracks, *J. Acoust. Soc. Am* **2002** (112), No. 6, 2567 – 2582, ISSN 1520-8524.

[7] V. Chmelko. Vrubové účinky v prevádzke strojov a konštrukcií, Vydavateľstvo STU, **2015**, ISBN 978-80-227-4482-9.

[8] V. Chmelko, V. Kliman, M. Garan. In-time monitoring of fatigue damage, *Procedia Engineering* **2015** (101), 93 – 100.

[9] M. Hlavatý, L. Starek. The detection of defects of mechanical structures using surface acoustic waves (SAW), *Engineering Mechanics* **2011**, Svratka, Czech Republic, 191 - 194

[10] L. Magdolen, M. Masaryk. Flywheel storage energy, *Conference Gepeszet 2012, May 24-25, 2012, Budapest, Hungary, Conference proceedings*, Budapest university of Technology and Economy BME Budapest, **2012**, ISBN 978-963-313-055-1.

[11] B. Masserey, P. Fromme. On the reflection of coupled Rayleigh-like waves at surface defects in plates, *J. Acoust. Soc. Am* **2008** (123), No. 1, 88 – 98, ISSN 1520-8524.

[12] B. Masserey, P. Fromme. Surface defect detection in stiffened plate structures using Rayleigh-like waves, *NDT&E International* **2009** (42), 564 – 572, ISSN 0963-8695.

[13] M. Musil. Crack localization and quantification, *Journal of Mechanical Engineering - Strojnícky časopis* **2001** (52), No. 2, 103 - 116, ISSN 0039-2472

[14] M. Musil. Localization and quantification of breathing crack. *Journal of Dynamic Systems Measurement and Control-Transactions of the ASME* **2006** (128), No. 2, 458 - 462, ISSN 0022-0434